energy&fuels

Article

pubs.acs.org/EF

In-Situ Transesterification of *Chlorella vulgaris* Using Carbon-Dot Functionalized Strontium Oxide as a Heterogeneous Catalyst under Microwave Irradiation

Alex Tangy,[†,#] Vijay Bhooshan Kumar,[†,#] Indra Neel Pulidindi,[†] Yael Kinel-Tahan,[‡] Yaron Yehoshua,[‡] and Aharon Gedanken*[,†]

[†]Department of Chemistry, Bar-Ilan University, Ramat-Gan 52900, Israel

[‡]The Mina and Everard Goodman Faculty of Life Sciences, Bar-Ilan University, Ramat-Gan 5290002, Israel

Supporting Information

ABSTRACT: The main goal of this study is to functionalize SrO with carbon dots (C-dots) and to explore the composite as a catalyst for fatty acid methyl esters (FAME) production using *Chlorella vulgaris* as feedstock. C-dots are synthesized by sonicating polyethylene glycol followed by sonochemical modification of $Sr(NO_3)_2$ (precursor for SrO) with C-dots. Sonication facilitates the adhesion of C-dots to the surface of $Sr(NO_3)_2$. The resulting material is calcined in an inert environment to form a SrO−C-dot composite. The effect of functionalizing SrO with C-dots on the transesterification of the lipids in the alga with methanol is studied. The optimization of a one-stage process of conversion of the lipid fraction of microalga *Chlorella vulgaris* into FAME using direct transesterification under microwave irradiation is illustrated. A lipid conversion value of 45.5 wt % is achieved using the SrO−C-dot catalyst after 2.5 min of microwave (MW) irradiation. The catalyst displayed better activity than commercial SrO. Microwave irradiation accelerates the disruption of the microalgal cells and facilitates the release of lipid content into the reaction medium. The catalyst is characterized by a variety of physicochemical techniques. The FAME product obtained from the alga is quantified using ^{1}H NMR spectroscopy. The new catalyst, namely, SrO−C-dot nanoparticles (NPs), yielded 97 wt % FAME from *Chlorella vulgaris* in 2.5 min of MW irradiation.

1. INTRODUCTION

Depletion of fossil fuels, environmental concerns, and growing energy requirements prompt the replacement of at least part of the petroleum-based fuels used for transportation by renewable energy sources. The transportation sector, representing 30% of the world's total energy consumption, is the largest energy-consuming sector after the industrial sector. Almost 60% of world's oil demand is for the transportation sector, which will probably be the most energy-demanding sector in the future.[1] Biodiesel produced from renewable biological sources has gained importance as an alternative energy source to fossil-based transportation fuels such as petrol and diesel.[2,3] Biodiesel is generally produced using vegetable oils as feedstock. The major drawback of using edible biomass as feedstock is that arable land is used to farm the oil seed crops, and this can lead to a food-vs-fuel-vs-land conflict. Moreover, it has been reported that a number of feedstock, such as algal oils, jatropha, and waste cooking oil, can reduce 60−90% of the biodiesel production cost.[4]

Microalgae are photosynthetic microorganisms capable of converting sunlight, atmospheric CO_2, and wastewater into a variety of high-energy molecules, including fatty acids (FA) and triacylglycerols (TAGs), the major feedstock used for biodiesel or FAME production.[5,6] Microalgae, also called third-generation fuel, are considered one of the most promising feedstock for biofuels.[7] The productivity of these photosynthetic microorganisms in converting CO_2 to carbon-rich lipids greatly exceeds that of agricultural oleaginous crops, without competing for arable land and food crops.[8] Microalgae can be grown on fresh or salt water, and even in a wastewater environment.[6] Recent advances present opportunities to develop microalgae as feedstock for biodiesel production in a sustainable and economical way within the next 10−15 years.[9,10] Microalgae can be cultivated from several aqueous systems, such as ponds and photobioreactors. Microalgae have the highest growth rates among all the photosynthetic organisms.[11] Approximately 46 tons of oil/hectare/year can be produced from diatom algae.[12] These characteristics make them an attractive feedstock for biodiesel production.

Algal biomass contains macromolecular proteins, polysaccharides, and lipids, along with inorganic components.[13] Only the lipid content is generally targeted for FAME production. FAME production from microalgae can be divided into three main stages: (a) cultivation, (b) harvesting, and (c) lipid extraction and transesterification for FAME production. The lipid content of microalgae is dependent on the microalgae species and cultivation conditions. Microalgae can accumulate approximately between 20 and 70% of lipid content from the dry biomass.[14] The usual method for extracting lipids from the whole algae biomass consists of mixing the microalgae with an organic solvent such as chloroform or hexane as cosolvent, or adopting other methods, such as using a functional membrane coated with a cationic polymer[15] or using ionic liquids.[16] The extracted microalgal lipids are then converted to FAME by

Received: September 29, 2016
Revised: November 22, 2016
Published: November 22, 2016

DOI: 10.1021/acs.energyfuels.6b02519
Energy Fuels 2016, 30, 10602−10610

transesterification using alcohol and a catalyst. Recently, a combination of lipid extraction and FAME conversion in a one-step process, called direct (*in situ*) transesterification, has been reported.[17] This methodology simplifies the production process and improves the FAME yield compared to the conventional lipid extraction step, that involves lipid loss. Moreover, the number of stages in the biodiesel production process are also reduced in the *in situ* extraction-based processes. Direct transesterification has several advantages, such as cell disruption, lipid extraction, and transesterification, in a single step, and it has been proved to be more useful than conventional methods.[18,19] The conventional two-step preparation of biodiesel from microalgae has several disadvantages compared to *in situ* transesterification, including operation complexity, a longer process time, high energy consumption, and relatively higher cost, which restrict the commercial production of biodiesel from microalgae. Higher FAME yield is obtained by the direct transesterification than in a two-stage process.[17,20] Moreover, direct transesterification provides energy-efficient and economical routes for biodiesel production.[20]

Despite the high conversion yields achieved using homogeneous catalysts such as NaOH, KOH, H_2SO_4, etc., catalysts may remain in the FAME phase, and therefore, a FAME refining or washing step is needed. In this sense, the use of heterogeneous catalysts is a suitable alternative, allowing easy separation of the final product and reusability. Metal-oxide materials play an important role in the catalytic reaction because of their obvious advantages, which include easy processing, low cost, and easy modification into composites. Chang et al. have reviewed different types of catalytic systems mediated by solid mixed metal-oxides for biodiesel production.[21] Among the metal-oxide catalysts, alkaline earth metal-oxides possess excellent basicity and exhibit significant activity and selectivity in the transesterification reaction.[22] Specifically, the use of SrO, despite its lower surface area[23] and the partial solubility of the metal ion in the reaction medium,[24] results in almost complete conversion of waste cooking oil into FAME in 10 s under microwave irradiation.[25,26] Moreover, all the lipids in dry *Nannochloropsis* microalgae are fully converted to FAME via direct transesterification of the microalgae in 5 min of microwave irradiation.[17]

The existence of both microalgae, catalyst dispersed in methanol, and FAME at the end of the transesterification reaction when a heterogeneous catalyst is used leads to diffusion constraints of various components present in the medium relative to the case when a homogeneous catalyst is used. This leads to lowering of the reaction rate. The reaction takes place in the interfacial region between the catalyst, lipids, and methanol. Thus, either a highly active catalyst or vigorous mixing is required to increase the area of interaction/contact between the two phases.

The use of metal-oxide as a host matrix for C-dots has opened a new technological gateway for the development of catalysts due to the novel inherent characteristics of carbon nanostructures as well as nanometal-oxides. It is expected that replacing the commercial micron-sized catalytic particles by nanosized particles of SrO and C-dots can lead to further improvement in the transesterification rate of the conversion of algal biomass. C-dots are a nanostructured material with a substantial fraction of carbon, oxygen, and hydrogen. Carbon dots are a kind of quasi-zero-dimensional nanomaterial. The three dimensions are all 10 nm or less in size, so that the mobility of the internal electrons is restricted within the nanoscale dimensions in all directions.[27] C-dots may be a promising catalytic material because of their high chemical stability and multifunctionality.[28]

The efficiency of FAME production from microalgae can be improved by the use of microwaves.[17] Microwave irradiation enhances the mass transfer rate between immiscible phases and also diminishes the reaction time.[18] Moreover, the FAME production rate and yield from wet microalgae biomass obtained through the one-step process using microwave irradiation are 6-fold and 1.3-fold higher than those obtained through the two-step process using conventional heating.[29]

Our main objective in using microwave irradiation for the conversion of algae to FAME is to reduce production costs and energy requirements while maximizing lipid productivity, increasing the utilization efficiency of the biomass by making use of all algal biomass components and reducing the process time. The current report focuses on the design of an innovative catalytic process for a single-step conversion of *Chlorella vulgaris* into FAME using microwave irradiation. The goal of our investigation is to develop a new active catalytic material for FAME production, namely, C-dot-modified by SrO obtained from $Sr(NO_3)_2$, and to study its physical, chemical, and catalytic properties. To the best of our knowledge, there are no reports on the use of the SrO−C-dot composite as a catalyst for FAME production from microalga. This study is a continuation of our recent work[30] on the synthesis of C-dots and the elucidation of their physicochemical properties.

2. EXPERIMENTAL SECTION

2.1. Chemical reagents. Polyethylene glycol-400 (PEG-400, 99.998%) and $Sr(NO_3)_2$ (≥99.0%) used as a precursor of SrO are purchased from Sigma-Aldrich, Israel. Strontium oxide (SrO) (99.5%) is purchased from Alfa Aesar. Isopropyl alcohol (99.7%), acetone, methanol, and chloroform are purchased from Bio Lab and are used as received.

2.2. Preparation of SrO-C-dots. Recently, we have reported the formation of ultrafine C-dots[30] by ultrasonication of PEG-400. The current synthesis (Figure 1) was performed as follows: (Step 1) 20 mL of polyethylene glycol (PEG-400) was transferred into a quartz test tube that had been dipped in a water/Si-oil bath at 70 °C. The tip of an ultrasonic transducer (Sonics and Materials Inc., USA, model VCX 750, frequency 20 kHz, AC voltage 230 V) was dipped in the solution, about 2 cm above the bottom of the test tube. Ultrasonic irradiation was applied with a sonication amplitude of 70% for 2.5 h. These

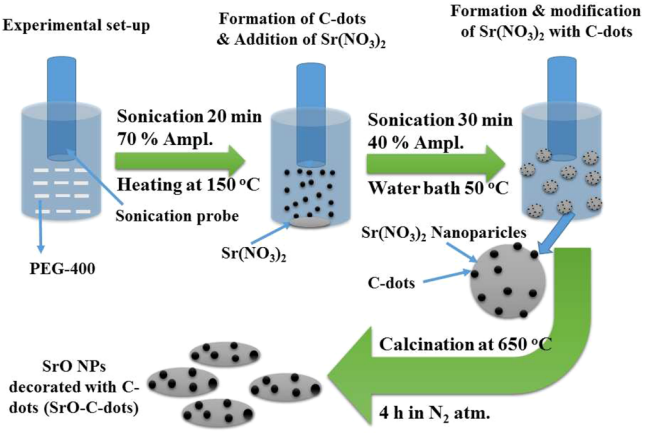

Figure 1. Schematic overview of the sonochemical synthesis of the $Sr(NO_3)_2$−C-dot composite.

DOI: 10.1021/acs.energyfuels.6b02519
Energy Fuels 2016, 30, 10602−10610

conditions are found to be optimal for the formation of C-dots.[30] (Step 2) 10 g of $Sr(NO_3)_2$ was added to the test tube, and the sonication was continued for another 30 min in a hot water bath at 50 °C. Subsequently, the product mixture was centrifuged. The $Sr(NO_3)_2$-C-dot nanoparticles were washed with double-distilled water and acetone (1:1) and then dried in vacuum at room temperature. The dried product was subjected to calcination for varying periods of time to determine the optimal conditions for the decomposition of $Sr(NO_3)_2$. The optimal condition was found by thermogravimetric analysis (TGA) measurements in the presence of N_2 gas. The calcination was performed in an inert atmosphere to prevent the decomposition of the C-dots. This methodology aided the *in situ* deposition of C-dots on the surface of $Sr(NO_{3)2}$ via sonication, and subsequent calcination of the material in an inert atmosphere resulted in the formation of a SrO−C-dot composite. The amount of carbon dots in the reaction medium is much lower than that of $Sr(NO_3)_2$ (10 g). In the calcined product, the relative amount of SrO (93 wt %) is much higher compared to that of carbon dots (7 wt %). Moreover, the particle size of SrO (20−40 nm) is greater than that of the carbon dots (7 nm). These factors confirm the possibility that SrO is a support upon which the carbon dots are functionalized in the composite material, SrO-C-dots.

2.3. Characterization of SrO−C-dots. The precise decomposition temperature of $Sr(NO_3)_2$−C-dot to SrO−C-dot was deduced from the TGA. The TGA curves were recorded using TGA-GC-MS (EI/CI) Clarus 680/Clarus SQ 8C by PerkinElmer over the temperature range 25−900 °C in both nitrogen and air atmospheres at a heating rate of 10 °C/min. Powder X-ray diffraction (PXRD) study is conducted to probe the crystallographic nature of the product (SrO-C-dot) and to verify the transformation of $Sr(NO_3)_2$ to SrO. XRD patterns were collected using a Bruker AXS Advance powder X-ray diffractometer (Cu Kα radiation; λ = 0.15417 nm) operating at 40 kV/30 mA with a 0.0019 step size per 0.5 s over the range of 10−80° (2θ). The phases were identified using the power diffraction file (PDF) database (JCPDS, International Centre for Diffraction Data). Fourier transform infrared (FT-IR) spectra are recorded in KBr pellet mode on a Nicolet (Impact 410) FT-IR spectrophotometer under atmospheric conditions. The samples are scanned over the range 400−4,000 cm^{-1}. The morphology of the C-dots−SrO composite and the respective elemental mapping is evaluated using high-resolution scanning electron microscopy (HR-SEM) with a JEOL-JSM 700F instrument and an LEO Gemini 982 field-emission gun SEM (FEG-SEM). Due to the low conductivity of SrO, the sample was coated with iridium (Ir). Elemental analysis was carried out using energy-dispersive X-ray spectroscopy (EDS) in conjunction with the HR-SEM instrument. Transmission electron microscopy (TEM) images of the SrO−C-dot particles are obtained using a Tecnai G2 (FEI, Oregon USA), a high-contrast/cryo TEM equipped with a bottom CCD 1 Kx1 K camera to visualize and evaluate the shape, size, and surface morphology of the SrO−C-dots. Samples for the TEM images were prepared by making a suspension of the particles in isopropyl alcohol, using water-bath sonication. Two small droplets of the sample containing SrO−C-dot particles are then applied on a TEM copper grid coated with a carbon film, and dried on a covered Petri dish in vacuum. The particle-size distribution of the SrO−C-dot nanoparticles is measured by the dynamic light-scattering (DLS) particle-size analysis model using a Zetasizer Nano SZ (Malvern Instruments Ltd., Worcestershire, UK). Raman spectra of the SrO−C-dots are recorded on a Renishaw inVia Raman microscope equipped with RL785 and RL830 Class 3B wavelength stabilized diode lasers and a Leica DM2500 M (Leica Microsystems) materials analysis microscope. A powder sample was sprinkled on the glass slide, and the Raman spectra were recorded. The fluorescence properties of the SrO-C-dots are studied with a Varian Cary Eclipse fluorescence spectrophotometer. The specific surface area of the particles was measured by the Brunauer−Emmett−Teller (BET) method at 77 K under liquid nitrogen on a Micromeritics instrument (Gemini 2375) after the samples were evacuated at 25 °C for 12 h with an evacuator (Micromeritics, Flow Prep 060).

2.4. Cultivation and harvesting of *Chlorella vulgaris*. Freshwater microalga *C. vulgaris* cultures are grown in the laboratory in a 3 L sterile flask using a Bristol medium (https://utex.org/products/bristol-medium), with air bubbling, under 70 μmol of photons m^{-2} s^{-1} and continuous LED light, at 22 °C with three replicates. After a week, the algae are transferred outdoors to a 30 L flat-panel photobioreactor (PBR). The light, temperature, oxygen, and pH were monitored with a computerized system for 12 days. The light is monitored with a Li-COR QUANTUM sensor; the temperature and dissolved oxygen are monitored by LDO sensors (HACH LANGE); the pH was monitored by pHD sc Digital Differential pH/ORP sensors (HACH LANGE). The daylight (12 h) reached up to 2,200−2,500 μmol photons m^{-2} s^{-1}. The temperature reached up to 29−42 °C at noon and 16−24 °C at night. The pH range was 6.1−7.8. During the first 7 days of the experiment, the initial inoculum reached maximum culture density. The nutrient deficiency diverted the biosynthesis toward lipid accumulation in the algae cells. The algal culture was harvested by centrifugation and freeze-dried in a lyophilizer.

2.5. *In-situ* transesterification of *Chlorella vulgaris*. The transesterification reaction was conducted under domestic microwave oven (DMWO) irradiation (Figure S1 in the Supporting Information). The DMWO was operated at 2.45 GHz in batch mode. The output of the domestic microwave reactor was 1,100 W. The microwave oven was operated at 70% power (cycle mode of 21 s on and 9 s off), a cycle mode function provided by the DMWO manufacturer. The microwave oven was modified to allow the distillation column to pass through it (for enhanced safety of operation) and a stirring facility during the reaction. The modification was performed by replacing the bottom part of the oven by a rounded aluminum plate. The plate was carefully attached to the framework in a manner that enables magnetic stirring. The reaction temperature obtained as a result of the microwave irradiation was measured using a Pyrometer (Fluke, 65 Infrared Thermometer) after the irradiation was completed. The reaction temperature was found to be 333 K immediately after completion of the irradiation.

The transesterification reactions are performed with a DMWO equipped with a condenser and carried out in a 50 mL round-bottom flask. A typical batch process of the transesterification reaction consists of taking 1 g of dried microalgae mixed with 10 mL of chloroform, 5 mL of MeOH (1:2 v/v) (based on the procedure of Folch et al.[31]), and 0.3 g of catalyst, SrO−C-dots, or commercial SrO, and irradiating the content in a microwave oven for a certain time. First, the catalyst was dispersed in MeOH by high magnetic stirring to ensure good dispersion of the catalyst into the MeOH. The microalgae and chloroform were subsequently added, and the mixture was irradiated. At the end of the reaction, the temperature of the mixture was measured with a pyrometer and was found to be 333 K, owing to the presence of the condenser, which allowed the cooling of the reaction. After the completion of the reaction, the samples were centrifuged and filtered under vacuum to separate the methanol−chloroform phase that contained the FAME from the residual microalgae, the glycerol, and the catalyst. The solution of methanol−chloroform was evaporated in a rotary evaporator, and the FAME content was determined gravimetrically.[17] The oil content was expressed by its weight relative to the weight of the microalgae biomass.

The FAME product is analyzed by ^{1}H NMR spectroscopy (Bruker Avance 300 spectrometer). Chloroform ($CDCl_3$) was used as a solvent for ^{1}H NMR sample preparation. The conversion is calculated directly from the integrated areas of the methoxy group in the FAME at 3.65 ppm (singlet) and from the integrated areas of the α-carbonyl methylene protons present in the triglyceride derivatives at 2.26 ppm (triplet). Equation 1 was used to estimate the conversion of the lipid content to FAME:

$$Conversion\ (\%) = \frac{2I_{Me}}{3I_{CH_2}} \times 100 \quad (1)$$

where I_{Me} is the integrated value of the protons of the methyl esters and I_{CH_2} is the integrated value of the methylene protons. The

DOI: 10.1021/acs.energyfuels.6b02519
Energy Fuels 2016, 30, 10602−10610

conversion ratio of the lipids in the microalgae to the resultant FAME was obtained by dividing I_{Me} by I_{CH_2}. The factors 2 and 3 were derived from the fact that methylene carbon possesses two protons and methyl carbon has three attached protons.[26]

3. RESULTS AND DISCUSSION

3.1. Characterization of SrO−C-dot catalyst. *3.1.1. Thermal analysis of $Sr(NO_3)_2$-C-dots and SrO-C-dot composite.* The TGA analysis of the $Sr(NO_3)_2$−C-dots before and after calcination for 4 h at 650 °C is shown in Figure 2. The TGA of

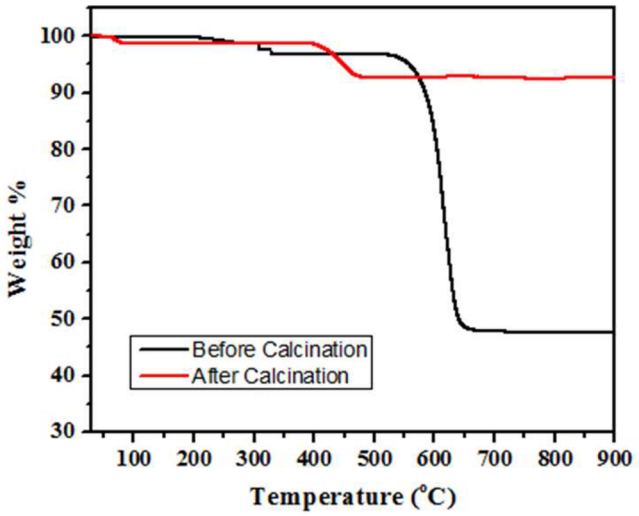

Figure 2. TGA curve of $Sr(NO_3)_2$−C-dots in N_2 atmosphere and of the SrO−C-dot composite in air after calcination of $Sr(NO_3)_2$−C-dots at 650 °C for 4 h in a N_2 environment at a constant heating rate of 10 °C/min.

the $Sr(NO_3)_2$-C-dots before calcination was performed in a nitrogen environment. The resulting material, SrO−C-dots, was further analyzed by TGA in an air atmosphere to evaluate the temperature decomposition of the C-dots. As indicated in Figure 2, in the case of the $Sr(NO_3)_2$−C-dots, the first weight loss (∼4 wt %) occurs between 200 and 325 °C due to dehydration and loss of water. The second and major weight loss (48.5 wt %) occurs between 650 and 660 °C, corresponding to the decomposition of the $Sr(NO_3)_2$ to SrO.[32] Pure $Sr(NO_3)_2$ melts at 571 °C and decomposes at 658 °C.[33] Our observation of the conversion of $Sr(NO_3)_2$ to SrO is consistent with the literature.[33] Moreover, the calcination temperature of 650 °C is reported as being the most suitable temperature for preparing solid-base catalysts from $Sr(NO_3)_2$, as a result of its thermal property.[32,34] The temperature must be high enough to decompose $Sr(NO_3)_2$ to the active oxide species, yet not high enough to hinder the sintering of the catalyst particles. Therefore, a calcination temperature of 650 °C was subsequently used for the decomposition of the $Sr(NO_3)_2$−C-dots to produce the SrO−C-dot catalyst. The TGA of the SrO−C-dot composite in air indicates a weight loss of 7% at ∼450 °C. The weight loss is attributed to the decomposition of the C-dots or the loss of OH, CO, and CO_2 from the surface functional groups of the C-dots. TGA analysis also confirms that the remaining 93 wt % is SrO and 7% is C-dots. Moreover, the plateau achieved at a temperature higher than 500 °C indicates the thermal stability of the SrO material. According to the decomposition formula of $Sr(NO_3)_2$ to SrO, the expected weight loss is 48.96 wt %, which is very close to the observed weight loss (48.5 wt %).

3.1.2. XRD analysis of SrO−C-dot composition and determination of calcination time. The crystal structure of the SrO−C-dot composite was analyzed using XRD. A calcination time of 2−3 h at 650 °C in a N_2 environment cannot completely convert all the $Sr(NO_3)_2$−C-dots to SrO−C-dots (Figure 3). Intense signals of a strontianite ($SrCO_3$)

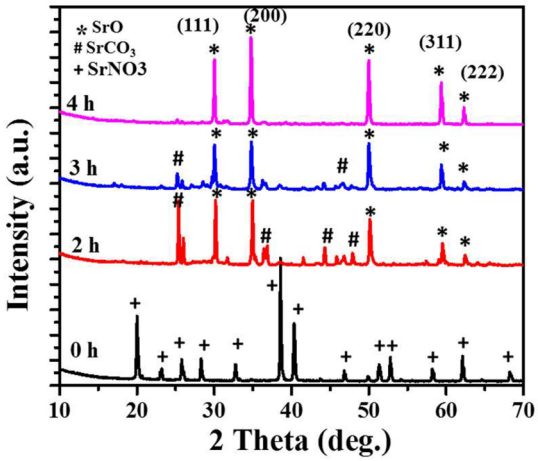

Figure 3. Effect of calcination time on the conversion of $Sr(NO_3)_2$−C-dots to SrO−C-dots (T = 650 °C; t = 1−4 h).

(JCPDF file no. 84-1778) with an orthorhombic phase belonging to a *Pmcn* space group were identified (2θ = 25.3°, 26.0°, 37.3°, 44.5°, 46.8°, and 48.0°) in addition to the SrO phase. The formation of strontianite is probably due to the reaction of the $Sr(NO_3)_2$ with the C-dots at elevated temperatures, even in an inert atmosphere, due to the high reactivity of the carbon dots. The $SrCO_3$ peaks are observed in the samples that were calcined for a period of over 3 h. However, the intensity of the peaks typical of $Sr(CO_3)_2$ decreases with increase in the calcination time. At the same time, the intensity of the signals corresponding to the oxide phase increased. A pure SrO phase is observed in the material after calcination for 4 h at 650 °C (JCPDF file no. 06-0520; cubic structure with a lattice constant value of 5.16 Å). The diffraction peaks at the 2θ values of 30.0°, 34.8°, 50.2°, 59.4°, and 62.4°, respectively, correspond to the (111), (200), (220), (311), and (222) planes of SrO. Signals typical of carbon structure were not observed at ∼25 and ∼45° due to the much smaller amount of carbon dots in the SrO−C-dot composite. Although, from the TGA analysis, the amount of carbon dots is ∼7 wt %, the carbon dots comprise elemental carbon, oxygen, and hydrogen existing as surface functional groups like the carboxyl and phenolic groups. Therefore, the actual amount of elemental carbon is even less than 7 wt %. This may be the reason for the absence of carbon signals in the XRD analysis (Figure 3). The FT-IR spectrum of the SrO−C-dots (Figure S2) shows a broad and strong absorption band at 592 cm^{-1}, with a shoulder at 620 cm^{-1} attributed to the Sr−O stretching vibration. The observed peak at 592 cm^{-1} attests to the formation of metal-oxide (Sr−O) bonds.[52,70,35] For comparison, commercial SrO was analyzed using FT-IR spectroscopy, and a significant attenuation of typical absorption bands is observed, probably due to the micron-sized particles of commercial SrO

DOI: 10.1021/acs.energyfuels.6b02519
Energy Fuels 2016, 30, 10602−10610

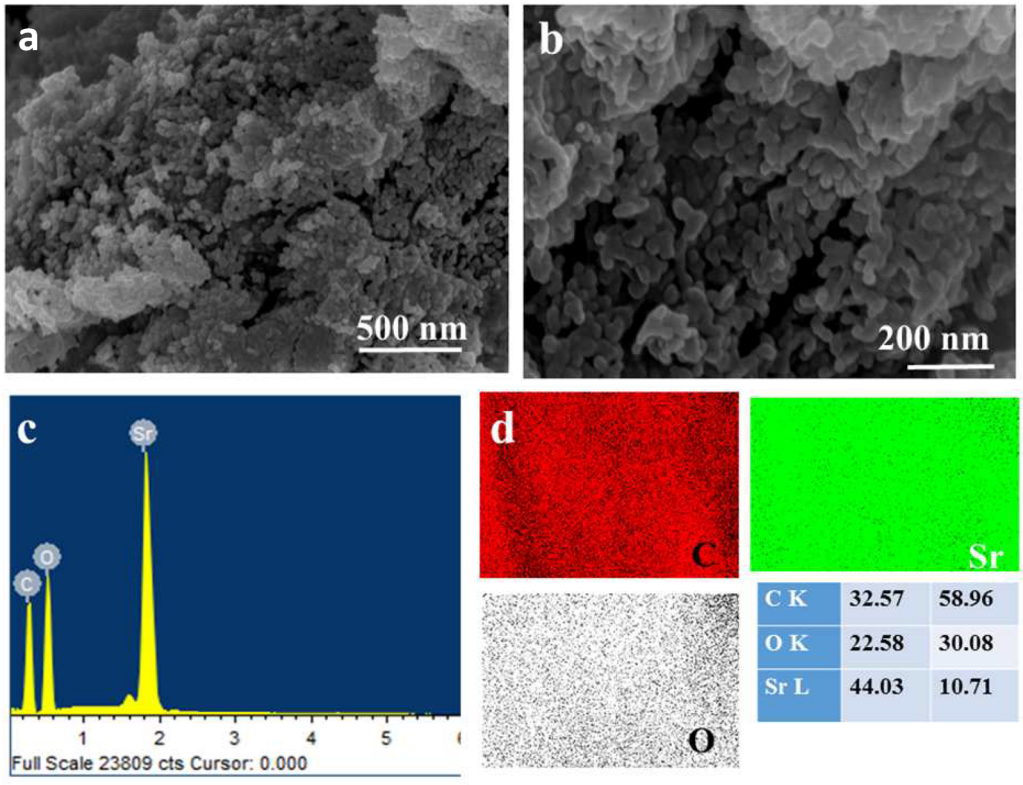

Figure 4. HR-SEM images (a and b), EDS spectrum (c), and elemental mapping (d) of the SrO−C-dot composite.

that absorb far less than the nanometric SrO powder in the SrO−C-dot composite.

3.1.3. Surface morphology and composition of the SrO−C-dot composite. The surface morphology of the SrO−C composite was deciphered from HR-SEM analysis, and the chemical composition of the composite was determined from EDS analysis. The SEM images, the EDS spectrum, and the elemental mapping recorded on the SrO−C-dot composite are shown in Figure 4. Functionalization of SrO with C-dots generates a high density of irregular small particles with a rough surface. In contrast, commercial SrO comprises large dense particles, exposing smooth planes or regularly faceted steps with micron-sized particles.[36] The results of the SEM analysis pertaining to the particle size and morphology of the SrO−C-dot composite are consistent with the BET sorptometry results. The specific surface area of the SrO−C-dot composite is 3.5 m^2 g^{-1}, whereas that of commercial SrO is 0.5 m^2 g^{-1}. The BET specific surface area value of the SrO−C-dot composite is 7 times greater than that of commercial SrO.[49] The particle size distribution of the catalyst was also evaluated by HRSEM, and the average particle size is 20−30 nm. Elemental mapping of the SrO−C-dot composite shows a uniform distribution of Sr, O, and elemental carbon on the surface. This indicates the complete decomposition of the $Sr(NO)_3$−C-dot to a SrO−C-dot composite as well as the homogeneous surface functionalization of SrO with carbon dots. The elemental composition shown by the EDS analysis is considered only for qualitative purposes and not as a quantitative estimate of carbon, owing to the fact that the analysis is carried out by spreading the sample on a carbon tape placed on a Cu stub.

3.1.4. TEM and DLS analysis of SrO-C-dots. The TEM image of SrO NPs surrounded by carbon dots displays a porous structure (Figure 5). The average particle size of carbon dots on

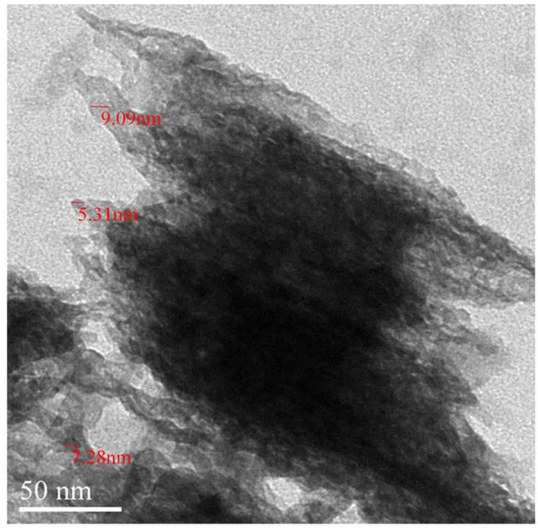

Figure 5. TEM of SrO−C-dot composite.

the SrO surface is ∼7 nm. The average particle size of the SrO is also measured in an isopropyl alcohol suspension by DLS (Figure S3). The suspension was formed using a bath sonicator. The results of the DLS analysis show that the size of the SrO particles in the composite is ∼200 nm. The particle size measured by DLS is about 10 times greater than that measured by HRSEM. The larger particle size values obtained by DLS measurement are due to particle aggregation.

3.1.5. Raman analysis. To confirm the presence of C-dots on the surface of SrO in the SrO−C-dot composite, Raman analysis was performed. Figure S4 shows the appearance of two prominent peaks at 1,380 and 1,549 cm^{-1}, corresponding to the D- and G-bands, respectively. The peak pattern is characteristic

DOI: 10.1021/acs.energyfuels.6b02519
Energy Fuels 2016, 30, 10602−10610

of the formation of carbon dots.[37] Moreover, in the case of the SrO−C-dot composite, the signal intensity of the graphitic G-band increases compared to the D-band, which is attributed to the increase in the crystallinity of the carbon structure formed at a high temperature calcination (650 °C for 4 h in an N_2 atmosphere), during which a variety of reactions, such as dehydration, cyclization, and condensation of the surface functional groups of carbon dots, can take place.

3.2. Evaluation of the catalytic activity of SrO−C-dots for the transesterification of lipids of *Chlorella vulgaris*.

The catalytic activity of the SrO−C-dot composite during the transesterification reaction is tested. A one-step direct transesterification reaction is carried out by irradiating the mixture of methanol and chloroform (1:2 v/v) and *Chlorella vulgaris* in the presence of SrO−C-dot catalyst in a domestic microwave oven at various irradiation times (2−5 min). The effect of the microwave irradiation time on the conversion of the lipids and the yield of FAME is depicted in Figure 6. A lipid conversion

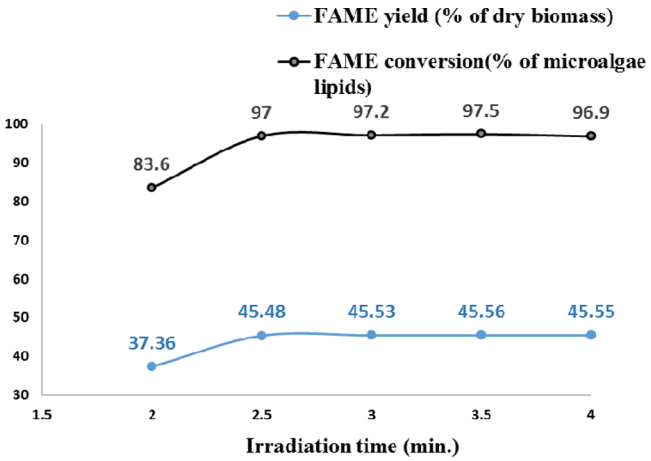

Figure 6. Effect of microwave irradiation time on FAME yield and conversion of lipids of *Chlorella vulgaris* to FAME using SrO−C-dot composite as catalyst.

value of 97 wt % and a corresponding FAME yield of 45.5 wt %, calculated gravimetrically, were achieved in a short reaction time of 2.5 min. The values of conversion of lipids and yield of FAME are achieved with a modest amount of catalyst (0.3 g), comprising 93 wt % SrO (0.279 g) and 7 wt % (0.021 g) C-dots.

For comparison, commercial micrometer-sized SrO particles were also used as the catalyst for the direct transesterification of *Chlorella vulgaris* under identical reaction conditions. A plot of the variation in the conversion of the lipid and the yield of FAME using a commercial SrO catalyst is depicted in Figure 7. With the commercial SrO catalyst, an irradiation time of 6 min is required to reach similar conversion and yield values obtained using the SrO−C-dot composite catalyst in 2.5 min. Thus, the transesterification is accelerated by approximately 2.4 times using the SrO−C-dot catalyst, indicating its improved performance over the conventional SrO catalyst. The improved activity of the SrO−C-dot composite for the acceleration of the transesterification of lipid content is attributed to the unique structural features of the C-dots. C-dots are extremely hydrophilic, owing to their extensive surface functionalization. Surface functionalities such as carboxylic and phenolic groups are acidic in nature. These moieties play a crucial role in the esterification of free fatty acids (FFA) in the algal biomass.

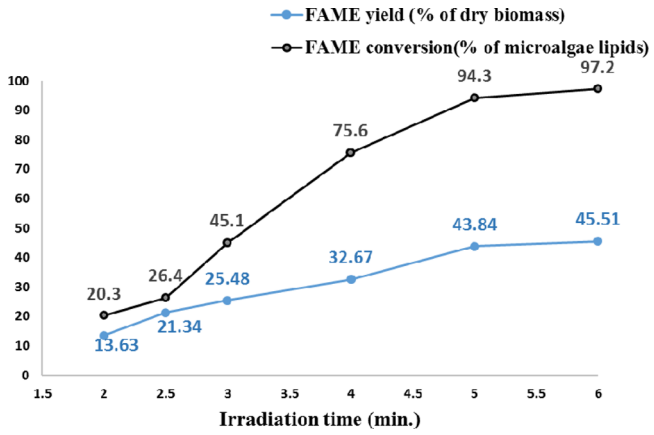

Figure 7. Effect of microwave irradiation time on FAME yield and conversion of lipids of *Chlorella vulgaris* to FAME using a commercial SrO catalyst.

Thus, the synergistic role of the acidic sites of the C-dots as well as the highly basic sites of SrO results in a 2.5-fold acceleration in the transesterification reaction compared to pure SrO. Another factor that is responsible for the enhanced activity of the SrO−C-dot composite is the surface area value, which is 7 times higher than that of commercial SrO.

A typical ^{1}H NMR spectrum of the FAME product obtained from *Chlorella vulgaris* using the SrO−C composite upon irradiation for 2.5 min is shown in Figure 8. The yield of FAME is estimated gravimetrically by calculating its weight relative to the weight of the dry microalgae biomass. The conversion percentage of oil to FAME is calculated by integrating the ^{1}H NMR peaks as shown in Figure 8 using eq 1. When SrO−C-dot composite is used as catalyst, optimal conversion is achieved after irradiation for 2.5 min, resulting in a FAME yield of 45.5%, which corresponds to the lipid conversion value of 97 wt %, as deduced from the ^{1}H NMR spectrum (Figure 8). Conversion values greater than 97 wt % could not be achieved even after irradiation for a longer time (Figure 6). This is probably due to the presence of residual FFA species in the microalgae.[38]

Besides the characteristic peak at 3.6 ppm, which arises from the methyl ester, and the triplet at 2.3 ppm related to the α-carbonyl methylene, which are characteristic peaks confirming the presence of methyl esters in FAME, the ^{1}H NMR spectrum shows a strong peak at 1.226 ppm arising from the methylene protons of the carbon chain of esters and a triplet at 0.851 ppm related to the terminal methyl-hydrogen protons. The other peak, which appears at 1.576 ppm, is attributed to β-carbonyl methylene protons.[39] The absence of a signal between 4.05 and 4.37 ppm in the ^{1}H NMR spectrum is attributed to the absence of CH_2 groups (−CH_2−O−COR) of triglycerides, indicating a high yield of FAME and high catalytic activity of the SrO−C-dots.[25] Thus, a novel composite of SrO and C-dots has been designed and tested for the accelerated production of FAME in a single step from *Chlorella vulgaris*.

Designing green and sustainable methods for extraction is a vital research topic in multidisciplinary areas. Recently, Crampon et al. reported effective extraction of neutral lipids from the microalgae *Spirulina platensis* using supercritical CO_2.[40] Chemat et al. introduced the concept of six principles of green-extraction that could be applied to an industrial process for intensification and energy savings[41] from the perspective of reduced energy consumption[26] and safe and high quality extraction of lipids from the algae using microwave

DOI: 10.1021/acs.energyfuels.6b02519
Energy Fuels 2016, 30, 10602−10610

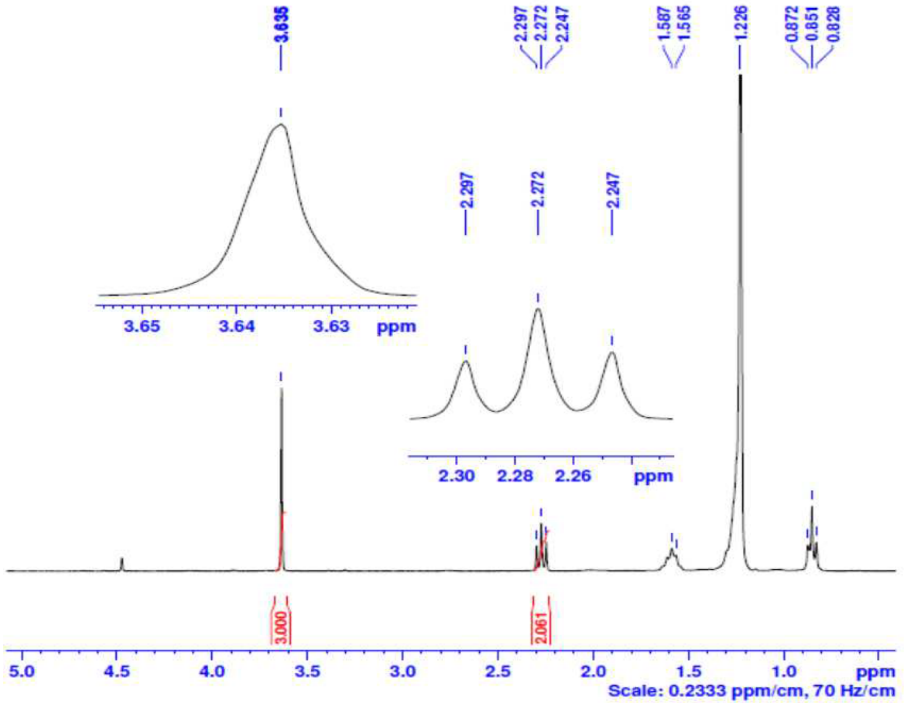

Figure 8. ^{1}H NMR spectrum of FAME obtained from the direct transesterification of *Chlorella vulgaris* by microwave irradiation for 2.5 min using the SrO−C-dot composite catalyst.

irradiation as well as ultrasonic waves. Even though microalgae is a versatile feedstock for biofuel production due to the tunability of the chemical composition (for instance obtaining high lipid content algae), higher productivity, and photosynthetic efficiency,[42−45] for the biodiesel production process to be sustainable and competitive, several challenges, such as resource constraints (CO_2, water, nutrients) and development of innovative large scale production technology, require immense research efforts and remain a challenge.[46−50]

4. CONCLUSION

A novel SrO−C-dot catalyst is prepared from $Sr(NO_3)_2$ and PEG400 as precursors for Sr and C, respectively, under sonochemical conditions. Homogeneous surface functionalization of SrO nanoparticles with carbon dots is achieved using the synthetic strategy developed based on sonication and subsequent calcination in an inert atmosphere at 650 °C for 4 h. The developed catalyst is used for the single-step conversion of *Chlorella vulgaris* to FAME in a microwave oven. A modest lipid conversion value of 97 wt % and a FAME yield of 45.5 wt % are achieved using the SrO−C-dot composite catalyst in a short reaction time of 2.5 min. The SrO−C-dot catalyst shows improved performance for the transesterification of lipids compared to the conventional SrO catalyst. The enhanced catalytic activity (2.4-fold) of the SrO−C-dot composite is attributed to the unique structural features of carbon-dots with a variety of oxygen, carboxylic, and phenolic functionalities that promote the esterification of FFAs in the algal biomass. Moreover, the higher surface area of SrO−C-dots compared to commercial SrO is another factor that enhances the catalytic activity with an increased number of accessible active reactant sites (lipids and MeOH). Thus, a SrO−C-dot composite catalyst is designed in an innovative way with very high potential for the fast and enhanced production of FAME from *Chlorella vulgaris*. This new methodology can be used for developing CaO/BaO/MgO−C-dot composites exclusively for biodiesel production.

■ ASSOCIATED CONTENT

Supporting Information

The Supporting Information is available free of charge on the ACS Publications website at DOI: 10.1021/acs.energyfuels.6b02519.

Image of the modified microwave oven (Figure S1), FT-IR spectra of SrO−C-dots and commercial SrO catalysts (Figure S2), dynamic light scattering (DLS) trace of SrO−C dot composite (Figure S3), and Raman spectra of C-dots and SrO−C-dot composite (Figure S4) (PDF)

■ AUTHOR INFORMATION

Corresponding Author

*Phone: 972-3-5318315; Fax: 972-3-7384053; E-mail: gedanken@mail.biu.ac.il.

ORCID

Aharon Gedanken: 0000-0002-1243-2957

Author Contributions

#Alex Tangy and Vijay Bhooshan Kumar have contributed equally to this work.

Notes

The authors declare no competing financial interest.

■ ACKNOWLEDGMENTS

Aharon Gedanken thanks the Israeli Ministry of Science, Technology and Space for the research grant (206712) supporting this work. Grateful thanks are due for the India−Israel cooperative scientific research grant (203768) supporting this research.

DOI: 10.1021/acs.energyfuels.6b02519
Energy Fuels 2016, 30, 10602−10610

REFERENCES

(1) Atabani, A. E.; Silitonga, A. S.; Badruddin, I. A.; Mahlia, T. M. I.; Masjuki, H. H.; Mekhilef, S. A Comprehensive Review on Biodiesel as an Alternative Energy Resource and Its Characteristics. *Renewable Sustainable Energy Rev.* **2012**, *16* (4), 2070−2093.

(2) Aransiola, E. F.; Ojumu, T. V.; Oyekola, O. O.; Madzimbamuto, T. F.; Ikhu-Omoregbe, D. I. O. A Review of Current Technology for Biodiesel Production: State of the Art. *Biomass Bioenergy* **2014**, *61*, 276−297.

(3) Luque, R.; Lovett, J. C.; Datta, B.; Clancy, J.; Campelo, J. M.; Romer, A. A. Biodiesel as Feasible Petrol Fuel Replacement: A Multidisciplinary Overview. *Energy Environ. Sci.* **2010**, *3*, 1706−1721.

(4) Baskar, G.; Aiswarya, R. Trends in Catalytic Production of Biodiesel from Various Feedstocks. *Renewable Sustainable Energy Rev.* **2016**, *57*, 496−504.

(5) Fu, C. C.; Hung, T. C.; Chen, J. Y.; Su, C. H.; Wu, W. T. Hydrolysis of Microalgae Cell Walls for Production of Reducing Sugar and Lipid Extraction. *Bioresour. Technol.* **2010**, *101* (22), 8750−8754.

(6) Leite, G. B.; Abdelaziz, A. E. M.; Hallenbeck, P. C. Algal Biofuels: Challenges and Opportunities. *Bioresour. Technol.* **2013**, *145*, 134−141.

(7) Foley, P. M.; Beach, E. S.; Zimmerman, J. B. Algae as a Source of Renewable Chemicals: Opportunities and Challenges. *Green Chem.* **2011**, *13* (6), 1399.

(8) Singh, B.; Guldhe, A.; Rawat, I.; Bux, F. Towards a Sustainable Approach for Development of Biodiesel from Plant and Microalgae. *Renewable Sustainable Energy Rev.* **2014**, *29*, 216−245.

(9) Wijffels, R. H.; Barbosa, M. J. An Outlook on Microalgal Biofuels. *Science (Washington, DC, U. S.)* **2010**, *329*, 796−799.

(10) Yan, X.; Tan, D. K. Y.; Inderwildi, O. R.; Smith, J. a. C.; King, D. a. Life Cycle Energy and Greenhouse Gas Analysis for Agave-Derived Bioethanol. *Energy Environ. Sci.* **2011**, *4* (9), 3110.

(11) Sharma, Y. C.; Singh, B.; Korstad, J. A Critical Review on Recent Methods Used for Economically Viable and Eco-Friendly Development of Microalgae as a Potential Feedstock for Synthesis of Biodiesel. *Green Chem.* **2011**, *13* (11), 2993−3006.

(12) Lin, L.; Cunshan, Z.; Vittayapadung, S.; Xiangqian, S.; Mingdong, D. Opportunities and Challenges for Biodiesel Fuel. *Appl. Energy* **2011**, *88* (4), 1020−1031.

(13) Savage, P. E. Algae Under Pressure and in Hot Water. *Science (Washington, DC, U. S.)* **2012**, *338* (6110), 1039−1040.

(14) Milano, J.; Ong, H. C.; Masjuki, H. H.; Chong, W. T.; Lam, M. K.; Loh, P. K.; Vellayan, V. Microalgae Biofuels as an Alternative to Fossil Fuel for Power Generation. *Renewable Sustainable Energy Rev.* **2016**, *58*, 180−197.

(15) Yoo, G.; Yoo, Y.; Kwon, J.-H.; Darpito, C.; Mishra, S. K.; Pak, K.; Park, M. S.; Im, S. G.; Yang, J.-W. An Effective, Cost-Efficient Extraction Method of Biomass from Wet Microalgae with a Functional Polymeric Membrane. *Green Chem.* **2014**, *16* (1), 312.

(16) Passos, H.; Freire, M. G.; Coutinho, J. A. P. Ionic Liquid Solutions as Extractive Solvents for Value-Added Compounds from Biomass. *Green Chem.* **2014**, *16* (12), 4786−4815.

(17) Koberg, M.; Cohen, M.; Ben-Amotz, A.; Gedanken, A. Bio-Diesel Production Directly from the Microalgae Biomass of Nannochloropsis by Microwave and Ultrasound Radiation. *Bioresour. Technol.* **2011**, *102* (5), 4265−4269.

(18) Hidalgo, P.; Toro, C.; Ciudad, G.; Navia, R. Advances in Direct Transesterification of Microalgal Biomass for Biodiesel Production. *Rev. Environ. Sci. Bio/Technol.* **2013**, *12* (2), 179−199.

(19) Nautiyal, P.; Subramanian, K. A.; Dastidar, M. G. Production and Characterization of Biodiesel from Algae. *Fuel Process. Technol.* **2014**, *120*, 79−88.

(20) Patil, P. D.; Reddy, H.; Muppaneni, T.; Mannarswamy, A.; Schuab, T.; Holguin, F. O.; Lammers, P.; Nirmalakhandan, N.; Cooke, P.; Deng, S. Power Dissipation in Microwave-Enhanced in Situ Transesterification of Algal Biomass to Biodiesel. *Green Chem.* **2012**, *14* (3), 809−818.

(21) Chang, F.; Zhou, Q.; Pan, H.; Liu, X.; Zhang, H.; Xue, W.; Yang, S. Solid Mixed-Metal-Oxide Catalysts for Biodiesel Production: A Review. *Energy Technol.* **2014**, *2* (11), 865−873.

(22) Yan, S.; Dimaggio, C.; Mohan, S.; Kim, M.; Salley, S. O.; Ng, K. Y. S. Advancements in Heterogeneous Catalysis for Biodiesel Synthesis. *Top. Catal.* **2010**, *53* (11−12), 721−736.

(23) Faungnawakij, K.; Yoosuk, B.; Namuangruk, S.; Krasae, P.; Viriya-empikul, N.; Puttasawat, B. Sr-Mg Mixed Oxides as Biodiesel Production Catalysts. *ChemCatChem* **2012**, *4* (2), 209−216.

(24) Nasreen, S.; Liu, H.; Khan, R.; Zhu, X. C.; Skala, D. Transesterification of Soybean Oil Catalyzed by Sr-Doped Cinder. *Energy Convers. Manage.* **2015**, *95*, 272−280.

(25) Koberg, M.; Abu-Much, R.; Gedanken, A. Optimization of Bio-Diesel Production from Soybean and Wastes of Cooked Oil: Combining Dielectric Microwave Irradiation and a SrO Catalyst. *Bioresour. Technol.* **2011**, *102* (2), 1073−1078.

(26) Tangy, A.; Pulidindi, I. N.; Gedanken, A. SiO 2 Beads Decorated with SrO Nanoparticles for Biodiesel Production from Waste Cooking Oil Using Microwave Irradiation. *Energy Fuels* **2016**, *30* (4), 3151−3160.

(27) Li, H.; Kang, Z.; Liu, Y.; Lee, S.-T. Carbon Nanodots: Synthesis, Properties and Applications. *J. Mater. Chem.* **2012**, *22* (46), 24230.

(28) Zheng, X. T.; Ananthanarayanan, A.; Luo, K. Q.; Chen, P. Glowing Graphene Quantum Dots and Carbon Dots: Properties, Syntheses, and Biological Applications. *Small* **2015**, *11* (14), 1620−1636.

(29) Cheng, J.; Yu, T.; Li, T.; Zhou, J.; Cen, K. Using Wet Microalgae for Direct Biodiesel Production via Microwave Irradiation. *Bioresour. Technol.* **2013**, *131*, 531−535.

(30) Kumar, V. B.; Porat, Z.; Gedanken, A. Facile One-Step Sonochemical Synthesis of Ultrafine and Stable Fluorescent C-Dots. *Ultrason. Sonochem.* **2016**, *28*, 367−375.

(31) Gossert, A. D.; Hinniger, A.; Gutmann, S.; Jahnke, W.; Strauss, A.; Fernandez, C. A Simple Protocol for Amino Acid Type Selective Isotope Labeling in Insect Cells with Improved Yields and High Reproducibility. *J. Biomol. NMR* **2011**, *51*, 449−456.

(32) Tantirungrotechai, J.; Thepwatee, S.; Yoosuk, B. Biodiesel Synthesis over Sr/MgO Solid Base Catalyst. *Fuel* **2013**, *106*, 279−284.

(33) Hosseini, S. G.; Eslami, A. Thermoanalytical Investigation of Relative Reactivity of Some Nitrate Oxidants in Tin-Fueled Pyrotechnic Systems. *J. Therm. Anal. Calorim.* **2010**, *101* (3), 1111−1119.

(34) Chen, W.; Huang, Z.; Liu, Y.; He, Q. Preparation and Characterization of a Novel Solid Base Catalyst Hydroxyapatite Loaded with Strontium. *Catal. Commun.* **2008**, *9* (4), 516−521.

(35) Rahman, M. M.; Hussain, M. M.; Asiri, A. M. A Novel Approach towards Hydrazine Sensor Development Using SrO·CNT Nanocomposites. *RSC Adv.* **2016**, *6* (70), 65338−65348.

(36) Yoosuk, B.; Krasae, P.; Puttasawat, B.; Udomsap, P.; Viriya-empikul, N.; Faungnawakij, K. Magnesia Modified with Strontium as a Solid Base Catalyst for Transesterification of Palm Olein. *Chem. Eng. J.* **2010**, *162* (1), 58−66.

(37) Wang, Q.; Liu, X.; Zhang, L.; Lv, Y. Microwave-Assisted Synthesis of Carbon Nanodots through an Eggshell Membrane and Their Fluorescent Application. *Analyst* **2012**, *137* (22), 5392−5397.

(38) Dong, T.; Wang, J.; Miao, C.; Zheng, Y.; Chen, S. Two-Step in Situ Biodiesel Production from Microalgae with High Free Fatty Acid Content. *Bioresour. Technol.* **2013**, *136*, 8−15.

(39) Monteiro, M. R.; Ambrozin, A. R. P.; Liao, L. M.; Ferreira, A. G. Determination of Biodiesel Blend Levels in Different Diesel Samples by 1H NMR. *Fuel* **2009**, *88* (4), 691−696.

(40) Crampon, C.; Nikitine, C.; Zaier, M.; Lepine, O.; Tanzi, C. D.; Vian, M. A.; Chemat, F.; Badens, E. Oil extraction from enriched *Spirulina platensis* microalgae using supercritical carbon dioxide. *J. Supercrit. Fluids* **2017**, *119*, 289−296.

(41) Chemat, F.; Vian, M. A.; Cravotto, G. Green extraction of natural products: Concept and principles. *Int. J. Mol. Sci.* **2012**, *13*, 8615−8627.

(42) Rajkumar, R.; Yaakob, Z.; Takriff, M. S. Potential of the micro and macro algae for biofuel production: A brief Review. *BioResources* **2014**, *9* (1), 1606−1633.

DOI: 10.1021/acs.energyfuels.6b02519
Energy Fuels 2016, 30, 10602−10610

(43) Dean, A. P.; Sigee, D. C.; Estrada, B.; Pittman, J. K.; Dean, A. P.; Sigee, D. C.; Estrada, B.; Pittman, J. K. *Bioresour. Technol.* **2010**, *101*, 4499−4507.
(44) Stockenreiter, M.; Graber, A. K.; Haupt, F.; Stibor, H. The effect of species diversity on lipid production by micro-algal communities. *J. Appl. Phycol.* **2012**, *24*, 45.
(45) Beevi, U. S.; Sukumaran, R. K. Cultivation of microalgae in dairy effluent for oil production and removal of organic pollution load. *Bioresour. Technol.* **2014**, *165*, 295−301.
(46) Stephens, E.; de Nys, R.; Ross, I. L.; Hankamer, B. *J. Pet. Environ. Biotechnol.* **2013**, *4*, 4.
(47) Hamawand, I.; Yusaf, T.; Hamawand, S. Growing algae using water from coal seam gas industry and harvesting using an innovative technique: A review and a potential. *Fuel* **2014**, *117*, 422−430.
(48) Shih, S. C. C.; Mufti, N. S.; Chamberlain, M. D.; Kim, J.; Wheeler, A. R. A droplet-based screen for wavelength-dependent lipid production in algae. *Energy Environ. Sci.* **2014**, *7*, 2366−2375.
(49) Yue, Z.; Ma, D.; Wang, J.; Tan, J.; Peng, S. C.; Chen, T. H. Goethite promoted anaerobic digestion of algal biomass in continuous stirring-tank reactors. *Fuel* **2015**, *159*, 883−886.
(50) San Pedro, A.; González-López, C. V.; Acién, F. G.; Molina-Grima, E. Outdoor pilot production of *Nannochloropsis gaditana*: Influence of culture parameters and lipid production rates in flat-panel photobioreactors. *Algal Res.* **2016**, *18*, 156−165.

DOI: 10.1021/acs.energyfuels.6b02519
Energy Fuels 2016, 30, 10602−10610